Available online on www.ijddt.com
International Journal of Drug Delivery Technology 2014; 5(3); 89-97

ISSN: 0975 4415

Research Article

Characterization, *In Vitro* Evaluation and Stability Studies of Indomethacin-Loaded Polyzwitterionic Copolymer Nanoparticles

Velichka Andonova[1*], George Georgiev[2], Stela Dimitrova[3], Mariana Katsarova[3], Margarita Kassarova[1]

[1]Department of Pharmaceutical Sciences, Medical University of Plovdiv, Bulgaria; [2]Faculty of Chemistry and Pharmacy, Sofia University "St. Kliment Ohridski", Sofia; [3]Department of Chemistry and Biochemistry, Medical University of Plovdiv, Bulgaria.

Available online: 30th September, 2015

ABSTRACT

The aim of the study was to investigate the influence of the nature and composition of the monomer feed, added to the reaction system indomethacin/vinyl acetate/3-dimethyl (methacryloyloxyethyl) aminopropyl sulfonate (IMC/VAc/DMAPS) and the characteristics of the obtained polymer latexes on indomethacin *In-situ* loading, its kinetic release properties, and drug stability. Indomethacin loaded nanoparticles were obtained by an emulsifier-free emulsion radical copolymerization of the monomers, in presence of the drug. Transmission electron microscopy, Attenuated Total Reflection Fourier Transform Infrared spectroscopic analyses, Particle size distribution and zeta potential analysis were carried out to characterize the *In-situ* loaded nanocarriers. High-performance liquid chromatography and UV/VIS spectroscopic analyses were applied to determine the drug loading, *In vitro* release properties and stability studies of the drug used.

High yield of 90 to 96% was obtained for the tested *In-situ* loaded nanocarriers. They possess a spherical shape with diameter ranging from 100 to 900 *nm* and zeta potential from -3.25 *mV* to -20.3 *mV*. Mono-modal and bi-modal particle size distribution was observed depending on monomer feed, added to the reaction system. It also influenced the drug loading and its release characteristics. Indomethacin was released from the investigated patterns following first order release. The nature and composition of the monomer feed, added to the reaction system IMC/VAc/DMAPS are an effective factors for the control of the indomethacin loading and also affect the rate and extent of drug-releasing but do not influence the kinetic model and drug transport mechanism. Stability studies indicated the stabilizing role of the polymer carrier on the *In-situ* included indomethacin.

Keywords: Indomethacin-loaded nanoparticles, radical polymerization, polyzwitterion nanoparticles, vinyl acetate co-polymers**.**

INTRODUCTION

Indomethacin (IMC), ([1-(4-chlorobenzoyl)-5-methoxy-2-methylindol-3-yl]-acetic acid) as a non-steroidal anti-inflammatory drug (NSAID) is well known. The FDA first approved IMC in January 1965. It is used for the treatment of inflammation caused by the rheumatoid arthritis, ankylosing spondylitis, gouty arthritis, osteoarthritis, and soft tissue injuries as tendinitis and bursitis. IMC blocks the enzymes cyclooxygenase 1 and 2 (COX-1 and COX-2) and thereby reduces the levels of prostaglandins. As a result, fever, pain and inflammation are reduced. Since IMC inhibits both COX-1 and COX-2, it inhibits the production of prostaglandins in the stomach and intestines, which maintain the mucous lining of the gastrointestinal tract. IMC along with its powerful anti-inflammatory action, therefore, like other non-selective COX inhibitors may cause peptic ulcers[1]. In this regard the control on the rate and extent of drug release from the dosage forms is of the utmost importance[2]. Furthermore, IMC is practically insoluble in water, unstable in alkaline and acidic media and slightly soluble in alcohol. In ophthalmology, IMC is used as topical eye drops for prevention of miosis during cataract surgery, cystoid macular edema and conjunctivitis[1]. Its use in liquid formulations is limited due to its insolubility in water, low bioavailability and ocular mucosa irritation.

Development of nanocarriers that deliver the drug specifically to the target site in order to meet the therapeutic needs of the patients at the required time and level remains the key challenge in the field of pharmaceutical biotechnology[3]. The nanocarriers could protect the drug from the adverse action of the environment and thus to improve its chemical stability. Furthermore, the carrier could influence the rate and extent of the drug release and thus also affect the bioavailability[4].

Polycaprolactone based nanoparticles (NPs) containing IMC and Argan oil have been fabricated for skin application and treatment of rheumatoid arthritis[5]. Good reproducibility, high drug loading and high values of zeta

**Author for Correspondence*

potential have been reported for the nanocarriers obtained via nanoprecipitation method.

The effect of Eudragit® L100, polyethylene glycol, and polysorbate 80 on encapsulation efficiency of IMC within enteric NPs has been studied[6]. Formulations were developed based on a multilevel factorial design (three factors, two levels). The amount of polyethylene glycol was shown to be the factor that had the greatest influence on the encapsulation efficiency (evaluated response) at 95% confidence level.

In another investigation a dramatic increase in the chemical stability and *In vitro* corneal permeability of IMC has been observed with the IMC-solid lipid NP formulation in comparison to the IMC solution- (0.1% w/v) and IMC hydroxypropyl-*ß*-cyclodextrin-based formulations (0.1% w/v)[7]. Compritol® 888 ATO has been selected as the lipid phase for the IMC-solid lipid NPs, as IMC exhibited highest distribution coefficient and solubility in this phase.

In a previous study the possibility of an effective incorporation of IMC into homopolymer poly(vinyl acetate) (pVAc) NPs[8] as well as mixtures of NPs of these polymers with the hydrophilic poly(3-dimethyl (methacryloyloxyethyl) aminopropyl sulfonate) (p(DMAPS)), Carbopol®[9], and chitosan[10] by one-stage emulsion polymerization without using an emulsifier was demonstrated for the first time. The challenge was to find easily available and feasible technological parameters for the effective control of the IMC release from the polymer NPs. For that purpose two approaches were tested. The first one was based on changes in the composition of polymer mixture (pVAc, pDMAPS, Carbopol® and chitosan) from which the NPs with included IMC were prepared[9,10]. With the second approach this control was based on the IMC inclusion in the copolymer of vinyl acetate (VAc) with 3-dimethyl (methacryloyloxyethyl) aminopropyl sulfonate (DMAPS) (p(VAc-co-DMAPS)) nanolatex and the control of the drug loading, encapsulation efficiency, and IMC kinetic release properties by the variation of the copolymer composition. The results of this approach are the subject of this work. The choice of DMAPS was based on its hydrophilic properties and polyzwitterionic character.

Stable copolymers of VAc and DMAPS in different mole ratios, obtained by emulsion radical polymerization of co-monomers, have been reported in the literature. Dry latex p(VAc-co-DMAPS) NPs have been used in the tableting of metoprolol tartrate, and verapamil hydrochloride to obtain a solid dosage form with sustained release[11-13]. Metoprolol tartrate has been included in copolymers of VAc and DMAPS by *In-situ* emulsion radical polymerization of the co-monomers[14].

The objective of this study was to investigate the influence of the nature and composition of the monomer feed, added to the reaction system (IMC/VAc/DMAPS) and the characteristics of the obtained polymer latexes on IMC *In-situ* loading, its kinetic release properties, and drug stability.

MATERIALS AND METHODS

In this research IMC (European Pharmacopoeia reference material) as a drug, vinyl acetate (VAc) as a monomer, and ammonium persulfate (AP) as an initiator were purchased from Fluka. DMAPS from Merck (Darmstadt, Germany) was used for obtaining p(VAc-co-DMAPS). Potassium dihydrogen phosphate and *di*-sodium hydrogen phosphate from Merck (Darmstadt, Germany) were used for preparation of phosphate-phosphate buffer (Sorensen's phosphate buffer) (PPB). It was used as a medium for *In vitro* dissolution study of IMC-p(VAc-co-DMAPS) NPs. All HPLC-grade solvents (methanol and acetonitrile) were obtained from Labscan (Ireland). HPLC-grade standards (indometacin and 4-Cl-benzoic acid) were purchased from Sigma (USA).

Preparation of IMC-p(VAc-co-DMAPS) NPs: IMC-p(VAc-co-DMAPS) NPs were obtained by an one-stage emulsifier-free emulsion radical copolymerization of VAc and DMAPS (v/v) (moll ratio 4:1, 1:1, and 1:4), in presence of IMC 1% (w/v). The polymerization was conducted in a nitrogen atmosphere and a temperature of 55°C, for 90 *min* under ultrasonic impact (Ultrasonicator Siel UST7.8-200, Gabrovo, Bulgaria). Ammonium persulphate (AP) in concentration 1% (w/v) was used as initiator. The model latexes were exposed on dialysis through membrane with MWCO 8000 *Da* for 7 *h* to eliminate the low molecular weight compounds (e.g. the initiator of process, residual monomers or free IMC) from the primary latex, and then the samples were freeze-dried[9,10]. NP yield (%Y) was calculated using the following equation[6,9,10]:

$$\%Y = \frac{\text{Total weight of NPs}}{\text{Weight of polymer} + \text{weight of IMC}} \text{x100} \quad (1)$$

Characterization of IMC-p(VAc-co-DMAPS) NPs

Transmission electron microscopy (TEM): TEM images of the investigated models were produced by transmission electron microscope JEOL JEM 2100 (JEOL Ltd., Japan) with accelerating voltage 200 *kV*. For the phase identification of the samples the diffraction mode of the microscope, Selected area electron diffraction (SAED), was used. The following preparation procedure was applied before the observation of the samples in the microscope: micro-quantities of the studied substance were mixed with distilled water in a test tube and placed in an ultrasonic bath to homogenise for 3 *min*. Thereafter, the suspension was dropped on carbon-coated standard Cu grid and dried on air conditions in a dust free environment for 24 *h*.

Attenuated Total Reflection Fourier Transform Infrared (ATR-FTIR) spectroscopic analyses: ATR-FTIR analyses was carried out with Nicolet™ iS ™ 10 FT-IR Spectrometer equipped with a Smart iTR™ Attenuated total reflectance sampling (diamond crystal) accessory (Thermo Scientific, Thermo Fisher Scientific, Inc., USA). The spectra were recorded from 4000 to 600 cm^{-1} using a DTGS detector. All spectra were corrected for H_2O and CO_2 using internal software.

Particle size distribution (PSD) and zeta potential (ZP) analysis: PSD and ZP analysis of tested models were

carried out with the apparatus Nanotrac Wave MN 401 (Microtrac, Inc., USA). The core methodology of the Nanotrac Wave is Dynamic Light Scattering, (DLS) incorporating the patented Controlled Reference Method for advanced power spectrum analysis of Doppler shifts under Brownian Motion. PSD of tested models was determined in measurement range of 0.8 *nm* - 6.54 *µm* (diameter), and minimum sample volume ~ 250 *µL*. ZP of tested models was determined in measurement range of +/-200 *mV*, size range 10 *nm* to 20 *µm* and less than 750 *µL*. Other specifications are: measurement angle 180°; repeatability 1% or better for 100 *nm* Polystyrene; concentration limits from *ppb* to 40% by volume in certain conditions; Laser Diode, 780 *nm*, 3 *mW* Nominal, no alignment required.

The samples were prepared using equal quantity of NPs Chromafil Xtra 1.00 *µm* before measuring the particle mean diameter and polydispersity index (PDI).

Drug loading and In vitro release studies

Drug loading assessment: Modification of HPLC assay of IMC and its related substances described by Tsvetkova *et al*. was used to determine the amount of incorporated IMC into the IMC-p(VAc-co-DMAPS) NPs[15]. The HPLC system was composed of a ProStar 230 solvent delivery module and PDA detector model 335, Microsorb-MV C18 column (150 *mm* × 4.6 *mm*, 5 *µm* particle size), all from Varian (Australia). A solvent system including methanol and acetonitrile in proportions 1:1 v/v (A) and H_2O with *pH*=3 (B) was used in isocratic condition 75A:25B. The flow rate was 1.1 *mL/min* and detection at 240 *nm*. The compound of interest was identified according to its retention time determined using authentic

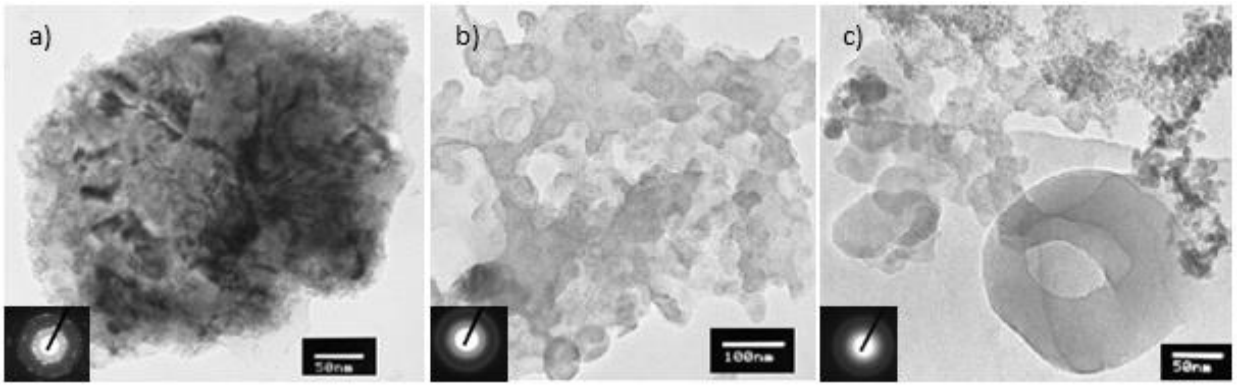

Figure 1: TEM of a) IMC-p(VAc-co-DMAPS)-1, b) IMC-p(VAc-co-DMAPS)-2, c) IMC-p(VAc-co-DMAPS)-3 and electron diffractions in the bottom left corner of the micrographs.

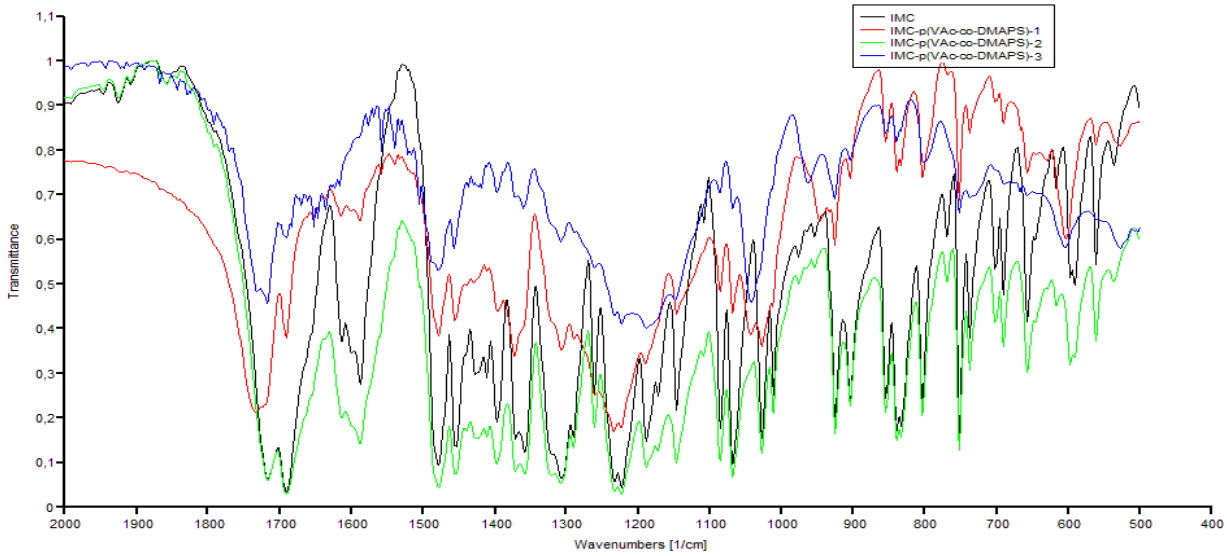

Figure 2: ATR-FTIR spectra of IMC, IMC-p(VAc-co-DMAPS)-1, IMC-p(VAc-co-DMAPS)-2, and IMC-p(VAc-co-DMAPS)-3.

in Sorensen's PPB at *pH* 7.4 and filtered through a filter IMC standard. It was quantified using an absolute

Table 1: Investigated models, moll ratio of co-monomers, and NP yield (%Y)

Model	Moll ratio VAc:DMAPS	%Y±SD
IMC-p(VAc-co-DMAPS)-1	4:1	92.78±0.76
IMC-p(VAc-co-DMAPS)-2	1:1	96.02±1.09
IMC-p(VAc-co-DMAPS)-3	1:4	90.45±0.65

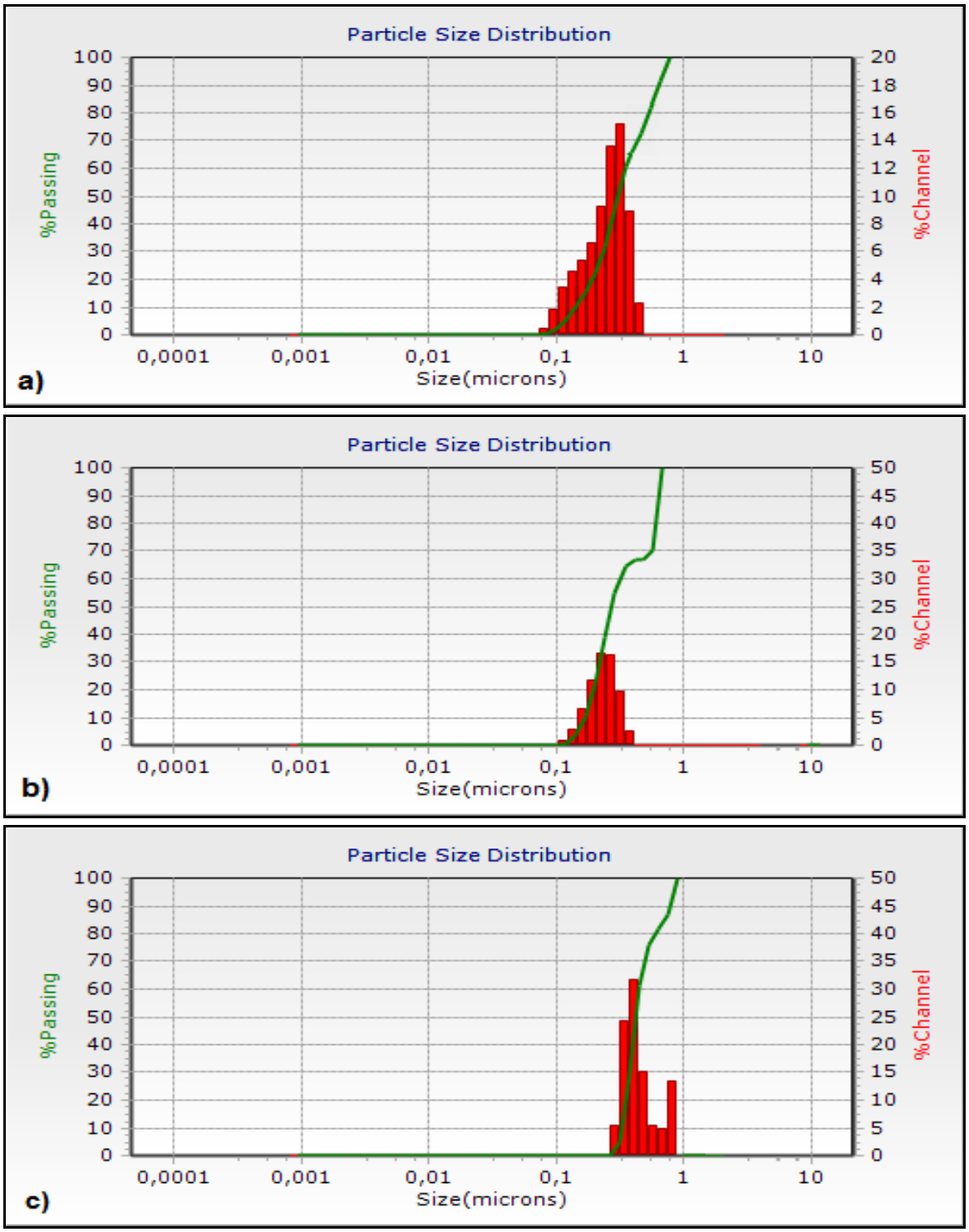

Figure 3: Particle size distribution of the tested models: a) IMC-p(VAc-co-DMAPS)-1; b) IMC-p(VAc-co-DMAPS)-2; c) IMC-p(VAc-co-DMAPS)-3.

calibration curve. Star Chromatography Workstation Version 6.30 (build 5) software was used.

The drug loading (%DL) and encapsulation efficiency (%EE) were calculated using the following equations[6,9,10]:

$$\%DL = \frac{\text{Weight of IMC entrapped within NPs}}{\text{Total weight of NPs}} \text{x}100 \quad (2)$$

$$\%EE = \frac{\text{Weight of IMC entrapped within NPs}}{\text{Total IMC added}} \text{x}100 \quad (3)$$

In vitro release of IMC from IMC-p(VAc-co-DMAPS) NPs: Examination on the release of IMC from the model nanosized particles was carried out in a thermostated vessel with equal amounts of the tested models under perfect "sink" conditions; working volume for dissolution 100.0 *mL* Sorensen's PPB at *pH* 7.4; temperature 37°C±0.5°C; stirring speed 100 min^{-1}. The quantitative defining of IMC was made spectrophotometrically at λ=320 *nm*[6,16] on UV/VIS spectrophotometer Ultrospec

Table 2: Encapsulation efficiency (%EE) and drug loading (%DL) of the tested models

Model	%EE±SD	%DL±SD
IMC-p(VAc-co-DMAPS)-1	25.50±0.31	2.50±0.11
IMC-p(VAc-co-DMAPS)-2	75.58±0.77	7.16±0.65
IMC-p(VAc-co-DMAPS)-3	15.50±0.44	1.56±0.11

SD – standard deviation, n=3

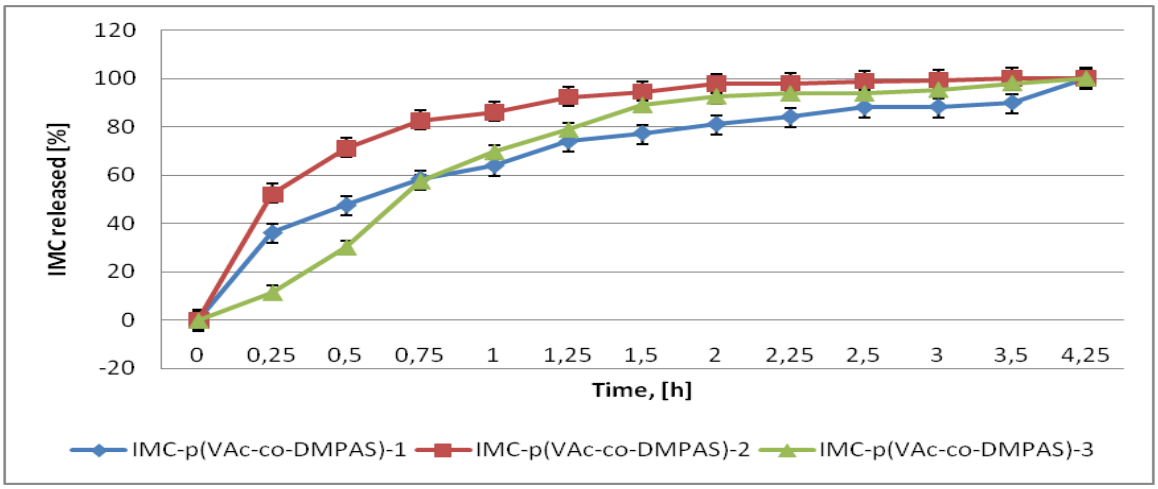

Figure 4: IMC release profiles from IMC-p(VAc-co-DMAPS)-1, IMC-p(VAc-co-DMAPS)-2, and IMC-p(VAc-co-DMAPS)-3 models.

Table 3: Correlation coefficient (R) values of different kinetic models for the IMC release from IMC-p(VAc-co-DMAPS)-NPs

Formulation	Correlation coefficient (R)			
	Zero order	First	Higuchi	Hixson-Crowell
IMC-p(VAc-co-DMAPS)-1	0.813	0.991	0.951	0.829
IMC-p(VAc-co-DMAPS)-2	0.626	0.995	0.973	0.638
IMC-p(VAc-co-DMAPS)-3	0.829	0.985	0.950	0.858

3300 pro (Biochrom Ltd., Cambridge, UK) after filtering the samples through a filter Chromafil Xtra 1.00 *μm*. The measurements were made compared to the medium of examination Sorensen's PPB at *pH* 7.4. Control experiments were performed using NPs without IMC. The concentrations were calculated from the standard curve with a linearity coefficient (r)=0.999.

Stability studies

Stability studies were conducted according to International Conference on Harmonisation (ICH) guidelines[17] and the WHO guidelines on the active pharmaceutical ingredient master file procedure[18].

Stress testing was carried out on a three primary batches of IMC-p(VAc-co-DMAPS)-2 NPs in an aqueous medium at *pH* 7.4 (Sorensen's PPB) under the conditions of elevated temperature (50, 60, and 70°C ± 2°C) and 75% ± 5% relative humidity (RH) for 8 *h*.

Long term study was conducted at 25°C ± 2°C/60% RH ± 5% RH with three primary batches of each tested dry models of IMC-p(VAc-co-DMAPS) NPs for 12 months.

HPLC analysis described above was used for the quantitative defining of IMC and 4-Cl-benzoic acid as a product of degradation of the drug used.

Statistical analysis

The data were analysed using the Statistical Package for the Social Sciences for Windows software, Version 11.0. Means were considered significantly different at $p < 0.05$. The results have been presented as the means of three experiments ± standard deviation.

RESULTS AND DISCUSSION

White or pale yellow coloured, finely dispersed powders of starting IMC-p(VAc-co-DMAPS) NPs were obtained by one stage emulsifier-free radical copolymerization of VAc and DMAPS (v/v) (moll ratio 4:1, 1:1, and 1:4), with *In-situ* included IMC 1% (w/v). The investigated models, moll ratio of co-monomers, and NP yield (%Y) are shown in Table 1. High yield of 90 to 96% was obtained for the tested IMC-p(VAc-co-DMAPS) models.

SD – standard deviation, n=3

Figure 1 shows TEM micrographs of the tested IMC-p(VAc-co-DMAPS) models. The particles of the observed samples possess a spherical shape, various sizes and different degree of aggregation. Model IMC-p(VAc-co-DMAPS)-1 (Fig.1a) was characterized with an irregular spherical shape and an approximate diameter 350-400 *nm*. A dense structure was observed with a drug dispersed in the polymer matrix of the NPs. In models

IMC-p(VAc-co-DMAPS)-2 (Fig.1b) and IMC-p(VAc-co-DMAPS)-3 (Fig.1c) spherical particles were observed, with different degree of dispersity, significantly smaller dimensions on the electronic photographs and non solid structure, compared to model IMC-p(VAc-co-DMAPS)-1 (Fig.1a). Figure 1 also shows a characteristic conformation in all tested models, resulting in a crystalline structure, demonstrated on the SAED patterns (in the bottom left corner of the micrographs). This effect can be explained by the crystallization of IMC itself, included in the nanosized particles, as it is confirmed by the XRD analysis[9] (the results are not shown). It is noteworthy that the SAED is a method for determination of a local structure, while XRD is for integral one.

The particles of the observed samples differ in size, shape and structure. The difference in the monomer feeding is essential on the morphological characteristics of the NPs obtained.

IMC-p(VAc-co-DMAPS)-1 was obtained in moll ratio of the monomers VAc:DMAPS = 4:1. The polymerization was conducted through the mechanism of an emulsifier-free emulsion copolymerization of VAc and DMAPS. The resulting latex particles were released into the aqueous phase. They have hydrophobic characteristics and would seek to obtain structures with the lowest surface energy - large particles with spherical shape (Fig.1a)[19].

IMC-p(VAc-co-DMAPS)-2 (Fig.1b) obtained in moll ratio of the monomers VAc:DMAPS = 1:1 shows a structure closer to that of the model IMC-p(VAc-co-DMAPS)-3 (Fig.1c). The micrograph on Fig.1b shows well-formed spherical NPs with dimensions around and under 100 *nm*. The structure is thicker than that of IMC-p(VAc-co-DMAPS)-3 (Fig.1c) and much lighter, more transparent than that of IMC-p(VAc-co-DMAPS)-1 model (Fig.1a).

IMC-p(VAc-co-DMAPS)-3 (Fig.1c) was obtained in moll ratio VAc:DMAPS = 1:4. There was no phase separation because of the four times greater amount of DMAPS. The system was homogeneous, and the copolymerization takes place as free-radical polymerization in an aqueous medium. The particles obtained are smaller than those of the model IMC-p(VAc-co-DMAPS)-1. They are distinguished by a lighter structure, and constitute hydrogels, swollen with water, which are difficult to separate from the aqueous phase. The electron diffraction photograph of this model strongly suggests the presence of IMC (Fig.1c, in the bottom left corner of the micrograph).

Drug–polymer compatibility is of essential importance in the design of pharmaceutical formulations, since therapeutic activity and/or bioavailability could be improved on the basis of their composition. Mid-infrared absorption spectroscopy has been widely used to study drug–polymer interactions[6]. In the present study ATR-FTIR spectroscopic analyses was carried out to demonstrate the interaction of IMC with the polymer nanocarriers.

Figure 2 shows the IR-spectra of the investigated models compared to the pure IMC. In the spectrum of pure IMC (γ–type is more stable and less soluble polymorphic modification of IMC in comparison with α-modification) two most intensive peaks, at 1717 cm^{-1} and at 1690 cm^{-1} of υC=O, are shown[20]. Spectrum of IMC-p(VAc-co-DMAPS)-2 model shows a greater similarity to this of pure IMC compared to the spectra of the other IMC-p(VAc-co-DMPS)-1 and IMC-p(VAc-co-DMAPS)-3 models[20,21]. Obviously, in the current systems there is no covalent interaction between polymers and IMC, but the interaction between them by hydrogen bonds is possible[21]. In the spectra of IMC-p(VAc-co-DMAPS)-1 and IMC-p(VAc-co-DMAPS)-3 there are the characteristic absorption peaks of IMC, but their intensity is much lower than those in the spectra of pure IMC and another investigated model because of the lower quantity of incorporated IMC in these NPs.

IMC-p(VAc-co-DMAPS) NPs obtained in different moll ratio of co-monomers VAc and DMAPS showed PSD, PDI, and ZP in wide range. The last one influences their behaviour in an aqueous environment and is related to the tendency of NPs to aggregate.

Fig. 3a shows PSD of model IMC-p(VAc-co-DMAPS)-1 in Sorensen's PPB at *pH* 7.4. NPs with dimensions below 100 *nm* and up to 700 *nm* (an average diameter 339.20±2.56 *nm*) and highest PDI 0.567 were found.

Narrower PSD was observed in the model IMC-p(VAc-co-DMAPS)-2 in the range of 100 *nm* to 600 *nm* (Fig. 3b) with PDI 0.198 and an average diameter 142.10±2.50 *nm*. Mono-modal PSD was observed for both models.

Model IMC-p(VAc-co-DMAPS)-3 was characterized with bi-modal PSD (Fig. 3c) in the diameter range of 400 *nm* up to 900 *nm* with PDI 0.381. The difference in the monomer feeding defines the hydrophilicity of the NPs. The particles in model IMC-p(VAc-co-DMAPS)-3, obtained in moll ratio VAc:DMAPS=1:4, were swollen hydrogels. TEM microphotography of this model (Fig.1c) confirms the presence of particles in a wide size range and suggests possible bi-modal PSD.

ZP values were -20.32±1.24 *mV* for IMC-p(VAc-co-DMAPS)-1, -12.50±0.32 *mV* for IMC-p(VAc-co-DMAPS)-2 , and -3.25±0.15 *mV* for IMC-p(VAc-co-DMAPS)-3, respectively.

The quantitative defining of IMC incorporated into the NPs was made according the HPLC analysis described above. A linear detection response was observed in concentration range between 0.50 and 8.00 *μg/mL* for IMC with correlation coefficient 0.9989.

Table 2 shows the results from drug loading assessment. Model IMC-p(VAc-co-DMAPS)-2 features with highest values for DL% and EE%. The monomers of DMAPS were dissolved in the aqueous medium, while the IMC was dissolved in the oil phase of VAc. Perhaps during the polymerization, under the influence of ultrasonic agitation of the system, droplets of the aqueous phase with dissolved DMAPS were included in the oil droplets of VAc with dissolved IMC. During the dialysis when the residues monomers and initiator AP were extracted and the subsequent lyophilization, pores were formed in the obtained NPs which help the inclusion of IMC in the carrier. That process also benefits the release of IMC.

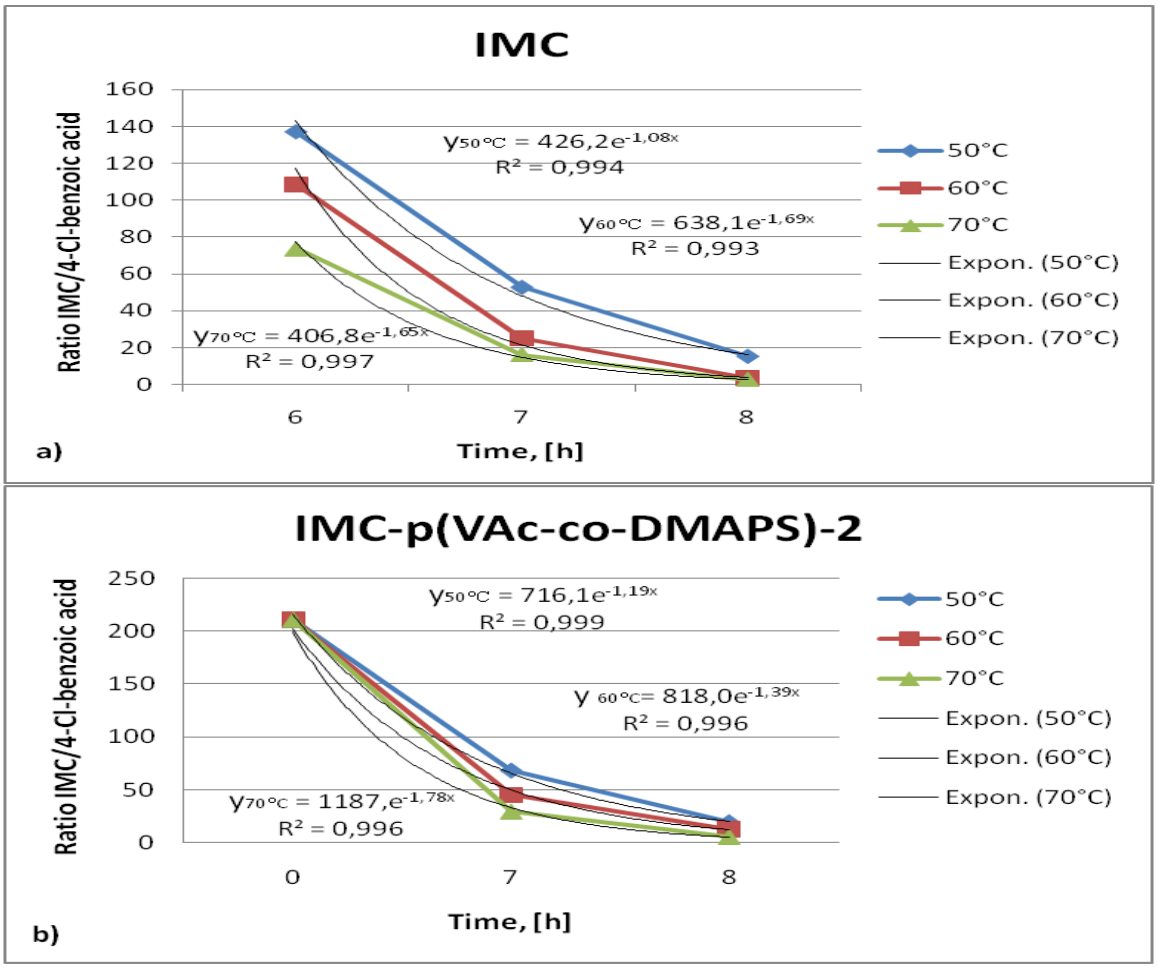

Figure 5: Ratio IMC/4-Cl-benzoic acid established in aqueous medium at pH 7.4 for a) IMC and b) for the IMC-p(VAc-co-DMAPS)-2 dispersions.

Therefore, the ratio 1:1 of the hydrophobic VAc to the hydrophilic DMAPS monomers resulted to the greatest extent on the incorporated drug. At IMC-p(VAc-co-DMAPS)-1 model, the fourfold lower content of DMAPS does not allow the creation of enough pores, which could incorporate IMC. At IMC-p(VAc-co-DMAPS)-3, the fourfold lower amount of VAc monomers prevents the dissolution of the drug and the formation of IMC-loaded NPs. That suggests predominantly inclusion of DMAPS in the formed IMC-p(VAc-co-DMAPS) NPs.

Figure 4 presents the release profiles of IMC included in the model carriers. The results are presented as a percentage of the IMC included into the NPs. Blank formulation has not any significant absorbance at 320 *nm*. The release profiles show the greatest speed and extent of IMC released for the same time from model IMC-p(VAc-co-DMAPS)-2 obtained at moll ratio of VAc:DMAPS =1:1.

Model IMC-p(VAc-co-DMAPS)-3 contains the least amount of IMC. In the first 45 *min* it releases the drug with the lowest speed and extent compared to the other models. After that the speed and extent of drug release becomes higher than model IMC-p(VAc-co-DMAPS)-1 and lower than model IMC-p(VAc-co-DMAPS)-2. These results could be explained with the swelling of the polymer carrier. After that period the extent and the speed of drug release in IMC-p(VAc-co-DMAPS)-3 increases compared to IMC-p(VAc-co-DMAPS)-1, where the less amount of pores formed slows the IMC release. In the first 45 *min* IMC-p(VAc-co-DMAPS)-1 releases the IMC located on the surface/surface pores of the NPs. Model IMC-p(VAc-co-DMAPS)-2 was characterized with the highest porosity. The formed pores facilitate not only the inclusion process, but also the release of the drug.

To determine the kinetic model that best describes the release mechanism, the *In vitro* release data were analyzed according to zero-, first-, Higuchi and Hixson-Crowell models. The model with the highest correlation coefficient (R) was selected as the best fit[22]. The results obtained show that IMC release from all investigated patterns follows the first order release kinetics (Table 3). These results relate to conditions in which there is no change in the shape of the NPs during the dissolution process (i.e. the surface area remains constant)[23]. Based on the high values of R for the Higuchi model it is possible to determine the drug transport mechanism as Fickian diffusion[24].

Stability studies

Stress testing was carried out on three primary batches of IMC-p(VAc-co-DMAPS)-2 NPs (as a promising model) in an aqueous medium at *pH* 7.40 (PPB) under the conditions of elevated temperature (50, 60, 70°C) and 75% relative humidity (RH) for 8 *h*. IMC solution was used as a control. Samples for analysis were taken at

specified intervals. The amount of IMC and 4-Cl-benzoic acid in the aqueous medium were determined via HPLC analysis, described above. A linear detection response was observed in concentration range between 0.50 and 8.00 *μg/mL* for IMC and 0.25 and 4.00 *μg/mL* for 4-Cl-benzoic acid with correlation coefficient 0.9989 and 0.9987 respectively. Figure 5 shows the ratio IMC/4-Cl-benzoic acid established in aqueous medium at *pH* 7.4 for IMC (Fig.5a) and for the IMC-p(VAc-co-DMAPS)-2 (Fig.5b) dispersions.

Traces of 4-Cl-benzoic acid as a breakdown product of the drug appear in the IMC solution on the 4th hour of the study for all the temperatures. Quantities of 4-Cl-benzoic acid, which can be determined by the HPLC method used, were determined at 6th hour of the study.

44.40±0.21 *μg/mL* IMC and 0.21±0.01 *μg/mL* 4-Cl-benzoic acid were established in the dry particles of the model IMC-p(VAc-co-DMAPS)-2 prior to heating (according drug loading assessment; ratio IMC/4-Cl-benzoic acid=211.43). This attitude was taken as a starting point of the presentation of the results from the nanocarriers. In the aqueous dispersion of model IMC-p(VAc-co-DMAPS)-2 quantities of 4-Cl-benzoic acid were established on the 7th hour of the study for all investigated temperatures. During this period of 7 hours change in the amount of IMC in the aquatic environment, connected with the process of drug release from the polymeric carrier, was only observed (the results are not presented).

Figure 5 shows that in the end of the study the ratio IMC/4-Cl-benzoic acid from IMC-p(VAc-co-DMAPS) dispersion was greater than the same from IMC dispersion at all of the tested temperatures. For example, the ratio IMC/4-Cl-benzoic acid from IMC-p(VAc-co-DMAPS) dispersion was 12.91 (4.26±0.21 *μg/mL* IMC and 0.33±0.02 *μg/mL* 4-Cl-benzoic acid) versus 3.67 (9.58±0.77 *μg/mL* IMC and 2.61±0.06 *μg/mL* 4-Cl-benzoic acid) from IMC dispersion at 60°C. The results from the study at 70°C were similar. The ratio IMC/4-Cl-benzoic acid from IMC-p(VAc-co-DMAPS) dispersion was 5.97 (4.30±0.32 *μg/mL* IMC and 0.72±0.04 *μg/mL* 4-Cl-benzoic acid) versus 2.68 (21.66±0.16 *μg/mL* IMC and 8.07±0.24 *μg/mL* 4-Cl-benzoic acid) from IMC dispersion. These results indicate the stabilizing role of the polymeric carrier on the IMC included. The data also suggest that the ratio IMC/4-Cl-benzoic acid was changed according to time-dependent exponential equation for all tested temperatures.

Long term study was conducted at 25°C ± 2°C/60% RH ± 5% RH with three primary batches of each tested dry models of IMC-p(VAc-co-DMAPS) NPs for 12 months. During the study it was not found increasing the quantity of the decomposition product and reducing the quantity of the drug more than 5%.

CONCLUSION

The results from this investigation definitely prove the importance of the properties of the components used in the polymerization system, on the properties and characteristics of the nanocarrier as a drug delivery system. The possibility for the *In-situ* IMC inclusion in the p(VAc-co-DMAPS) latexes was proved. IMC, as a hydrophobic drug, was released from the investigated patterns following first order release kinetics and it relates to conditions in which there is no change in the shape of the NPs during the dissolution process (i.e. the surface area remains constant). The addition of DMAPS monomer units in copolymer p(VAc-co-DMAPS) affects the rate and extent of IMC release but does not influence the kinetic model and drug transport mechanism. It was also shown that the composition of the copolymers was an effective factor for the control latex loading with IMC and its release characteristics. Stability studies indicated the stabilizing role of the polymer carrier on the *In-situ* included IMC.

The sustained release of the drugs used from copolymer zwitterionic matrix tablets has been demonstrated from the literature data[11-13]. The results from the present study strongly confirm the potential use of p(VAc-co-DMAPS) NPs as a drug delivery system not only for hydrophilic[14] but also for hydrophobic medicines. The co-monomer composition and physicochemical properties of the drugs in *In situ* loaded polyzwitterionic copolymer NPs define their controlled release characteristics. The change of co-monomer composition has proved easily available and feasible technological parameter for the effective control of the drug release from the polymer NPs.

Future investigations will concern the influence of the nature and quantity of other co-monomers on the controlled release characteristics of the drug used.

ACKNOWLEDGMENTS

The authors are grateful to the National Science Foundation (Project DDVU-02/43) and to Medical University of Plovdiv (Project HO-13/2013) for the financial support.

REFERENCES

1. Brayfield A. Martindale: The complete drug reference. Edn 38, London, Pharmaceutical Press, 2014.
2. Varma MVS, Kaushal AM, Garg A, Garg S. Factors affecting mechanism and kinetics of drug release from matrix-based oral controlled drug delivery systems. American Journal of Drug Delivery 2004; 2(1):43-57.
3. Rawat M, Singh D, Saraf S, Saraf S. Nanocarriers: promising vehicle for bioactive drugs. Biol Pharm Bull. 2006; 29(9):1790-8.
4. Chiappetta DA, Sosnik A. Poly(ethylene oxide)-poly(propylene oxide) block copolymer micelles as drug delivery agents: Improved hydrosolubility, stability and bioavailability of drugs. Eur J Pharm Biopharm. 2007; 66:303-17.
5. Badri W, Miladi K, Eddabra R, Fessi H, Elaissari A. Elaboration of nanoparticles containing indomethacin: Argan oil for transdermal local and cosmetic application. Journal of Nanomaterials 2015; ID 935439.
6. Dupeyrón D, Kawakami M, Ferreira AM, Cáceres-Vélez PR, Rieumont J, Azevedo RB, Carvalho JCT. Design of indomethacin-loaded nanoparticles: effect

of polymer matrix and surfactant. International Journal of Nanomedicine 2015; 8(1):3467-77.
7. Hippalgaonkar K, Adelli GR, Hippalgaonkar K, Repka MA, Majumdar S. Indomethacin-loaded solid lipid nanoparticles for ocular delivery: development, characterization, and *In Vitro* evaluation. J Ocul Pharmacol Th 2013; 29(2):216-28.
8. Andonova V, Georgiev G, Toncheva V, Kassarova M. Preparation and study of Poly(vinyl acetate) and Poly(styrene) nanosized latex with Indometacin. DiePharmazie 2012; 67(7):601-4.
9. Andonova V, Georgiev G, Toncheva V, Petrova N, Karashanova D, Penkov D, Kassarova M. Indomethacin Loading and *In Vitro* Release Properties from Vinyl Acetate Homo- and Co-Polymer Nanoparticles, Coated with Polyzwitterion and Carbopol® Shells. Int J Pharm Pharm Sci 2014; 6(1):691-9.
10. Andonova V, Georgiev G, Toncheva V, Karashanova D, Katsarov P, Kassarova M. Carbopol® and Chitosan Coated Nanoparticles with *In-Situ* Loaded Indomethacin. American Journal of PharmTech Research 2014; 4(1): 664-78.
11. Kostova B, Rachev D. New co-polymer zwitterionic matrices for sustained release of verapamil hydrochloride. Acta Pharm. 2007; 57: 429-439.
12. Kamenska E, Kostova B, Ivanov I, Rachev D, Georgiev G. Synthesis and Characterization of Zwitterionic Co-polymers as Matrices for Sustained Metoprolol Tartrate Delivery. Journal of Biomaterials Science, Polymer Edition 2009; 20(2):181-97.
13. Kostova B, Kamenska E, Ivanov I, Momekov G, Rachev D, Georgiev G. Verapamil hydrochloride Release Characteristics from new Copolymer Zwitterionic Matrix Tablets. Pharm. Dev. Tech. 2008.
14. Kostova B, Kamenska E, Rachev D, Simeonova S, Georgiev G, Balashev K. Polyzwitterionic copolymer nanoparticles loaded *in situ* with metoprolol tartrate: synthesis, morphologyand drug release properties. J Polymer Res 2013; 20:60.
15. Tsvetkova B, Pencheva I, Zlatkov A, Peikov P. High performance liquid chromatographic assay of indomethacin and its related substances in tablet dosage forms. Int J Pharm Pharm Sci 2012; 4(3):549–52.
16. Tzankov B, Yoncheva K, Lambov N. Development of carbopol-coated Indometacin loaded poly (lactide-co-glycolide) nanoparticles. Pharmacia 2013; 60(2):3-7.
17. International Conference on Harmonisation. *ICH Q1A* (*R2*)*:* Stability testing of new drug substances and products (http://www.ich.org/LOB/media/ MEDIA419.pdf).
18. Guidelines on active pharmaceutical ingredient master file procedure. In: WHO Expert Committee on Specifi cations for Pharmaceutical Preparations. Forty-second report. Geneva, World Health Organization, 2008, Annex 4 (WHO Technical Report Series, No. 948).
19. Yamak HB. Emulsion Polymerization: Effects of Polymerization Variables on the Properties of Vinyl Acetate Based Emulsion Polymers. Chapter 2, INTECH, 2013.
20. Rezaei Mokarram A, Kebriaee zadeh A, Keshavarz M, Ahmadi A, Mohtat B. Preparation and in-vitro evaluation of indomethacin nanoparticles. DARU 2010; 18(3).
21. Zlatkov A, Peikov P, Obreshkova D, Pencheva I. Spectral analyses methods for chemical compounds. Macros, Plovdiv, 2010.
22. Ibrahim MM, Abd-Elgawad A-E H, Soliman O A-E, Jablonski MM. Natural bioadhesive biodegradable nanoparticles-based topical ophthalmic formulations for sustained celecoxib release: in vitro study. Journal of Pharmaceutical Technology and Drug Research 2013; 2:7.
23. Singhvi G, Mahaveer S. In-vitro drug release characterization models. IJPSR. 2011; II(I):77-84.
24. Collett J, Moreton R. Formulation of modified-release dosage forms. In Aulton's Pharmaceutics. Edited by Aulton M, Edn III, Churchill Livingstone Elsivier, 2007